

EFFECTS OF NEUTRINO-DRIVEN KICKS ON THE SUPERNOVA EXPLOSION MECHANISM

CHRISTOPHER L. FRYER^{1,2} AND ALEXANDER KUSENKO³

Received 2005 November 10; accepted 2005 December 26

ABSTRACT

We show that neutrino-driven pulsar kicks can increase the energy of the supernova shock. The observed large velocities of pulsars are believed to originate in the supernova explosion, either from asymmetries in the ejecta or from an anisotropic emission of neutrinos (or other light particles) from the cooling neutron star. In this paper we assume the velocities are caused by anisotropic neutrino emission and study the effects of these neutrino-driven kicks on the supernova explosion. We find that if the collapsed star is marginally unable to produce an explosion, the neutrino-driven mechanisms can drive the convection to make a successful explosion. The resultant explosion is asymmetric, with the strongest ejecta motion roughly in the direction of the neutron star kick. This is in sharp contrast with the ejecta-driven mechanisms, which predict the motion of the ejecta in the opposite direction. This difference can be used to distinguish between the two mechanisms based on the observations of the supernova remnants.

Subject heading: supernovae: general

Online material: color figures

1. INTRODUCTION

Current observations of pulsar proper motions suggest that a large fraction of neutron stars are moving with velocities in excess of 400 km s^{-1} (Cordes & Chernoff 1998; Fryer et al. 1998; Lai et al. 2001; Arzoumanian et al. 2002). The large energy and momentum released during the formation of the neutron star (and the ensuing supernova explosion), coupled with the growing evidence that many core-collapse supernovae exhibit asymmetric explosions, has led to a general consensus in astronomy that neutron stars receive these large “kicks” at birth. But a number of mechanisms exist to try to explain the pulsar motions.

Evolution of close binaries has been considered as a possible origin of the pulsar kicks (Gott et al. 1970). If one of the stars in the binary system undergoes a supernova explosion, the binary system can be disrupted, producing runaway stars with high velocities. Many binary systems have orbital velocities as high as $100\text{--}200 \text{ km s}^{-1}$, but this is still too low a speed for explaining the average pulsar speed. This proposal was also criticized by Trimble & Rees (1971) for other reasons: the more evolved member of a binary system should have a lesser mass, and its explosive ejection should not disrupt the system.

An asymmetric emission of radio waves could occur if the pulsar’s dipole magnetic field is off-centered and inclined to the axis of rotation. Harrison & Tademaru (1975) have suggested that such radio waves could accelerate the newly born pulsar. However, the predicted final velocity falls short of the observed speeds of the faster pulsars, which exceed 1000 km s^{-1} . The failure of these two mechanisms leaves us with mechanisms occurring in the collapse phase itself. These mechanisms can be separated into two classes: ejecta-driven kicks and the kicks driven by emission of neutrinos or other weakly interacting particles.

Ejecta-driven kicks can occur if a sufficient degree of anisotropy develops in the hydrodynamics of the explosion. Since only 1% of the collapse energy accompanies the ejecta, large asymmetries are required to produce large supernova kicks. A

number of ejecta asymmetries have been proposed: asymmetric collapse (Burrows & Hayes 1996), low mode convection (Herant et al. 1992; Buras et al. 2003), and the related low-mode convection in an accretion shock instability (Blondin et al. 2003). Asymmetries in the progenitor star cannot produce kicks in excess of 200 km s^{-1} (Fryer 2004), far short of the observed 1000 km s^{-1} . Asymmetries produced by low mode convection has proven more successful (Buras et al. 2003) in two-dimensional studies. Such mechanisms require, by momentum conservation, that the kick be along the explosion asymmetry, but moving in the opposite direction of the ejecta.

Asymmetric neutrino emission has been proposed as an alternate kick mechanism. This mechanism takes advantage of the fact that most of the energy and momentum released in the collapse of a massive star is in the form of neutrinos, and asymmetries of a percent are sufficient to produce the observed kicks. The proposed mechanisms range from collective effects, for example, turbulence near the neutrinosphere (Socrates et al. 2005), to elementary processes involving neutrinos, including neutrino oscillations (Kusenko & Segré 1996, 1997; Barkovich et al. 2002, 2004; Fuller et al. 2003; Kusenko 2004). All these mechanisms require strong magnetic fields. Although the surface magnetic fields of ordinary radio pulsars are estimated to be of the order of $10^{12}\text{--}10^{13} \text{ G}$, the magnetic field inside a neutron star may be much higher, probably as high as 10^{16} G (Blandford et al. 1983; Duncan & Thompson 1992; Thompson & Duncan 1993; Kouveliotou et al. 1999).

Naively, one might think that even the standard Urca reactions responsible for production of neutrinos, $p + e^- \rightleftharpoons \nu_e + n$ and $\bar{\nu}_e + p \rightleftharpoons n + e^+$, have a sufficient asymmetry to give the neutron star a kick. Indeed, the rates of the Urca processes depend on the relative orientations of the electron spins and the neutrino momentum. Hence, there is a 10%–20% anisotropy in the distribution of neutrinos in every one of these processes (Chugai 1984; Dorofeev et al. 1985). However, this asymmetry in production does not lead to any asymmetry in the emission of neutrinos, because the anisotropy is washed out by the rescattering of neutrinos on their way out of the star (Vilenkin 1995; Kusenko et al. 1998; Arras & Lai 1999). If some other particles, with interactions weaker than those of neutrinos were produced anisotropically, their emission would remain anisotropic. For example,

¹ Department of Physics, University of Arizona, Tucson, AZ 85721.

² Theoretical Division, Los Alamos National Laboratory, Los Alamos, NM 87545.

³ Department of Physics and Astronomy, UCLA, Los Angeles, CA 90095-1547.

if sterile neutrinos exist and have a small mixing with active neutrinos, they should be produced in the Urca processes at the rate suppressed by the square of the mixing angle (Fuller et al. 2003). It is intriguing that the parameters of the sterile neutrinos required for the pulsar kicks (Kusenko & Segré 1997; Fuller et al. 2003) are consistent with the mass and mixing that make the sterile neutrino a good dark matter candidate (Fuller et al. 2003).

There is strong evidence that most of the gravitating matter in the universe is not made of ordinary atoms. This evidence is based on a consensus of observations of galaxy rotation curves, cosmic microwave background radiation, gravitational lensing, and X-ray emission from galaxy clusters. None of the known particles can be the dark matter, and a number of candidates have been proposed. Perhaps the simplest extension of the standard model that makes it consistent with cosmology is the addition of a sterile neutrino with a 2–15 keV mass. Unlike the active fermions, which must be added in the whole generations to satisfy the anomaly constraints, or the supersymmetric particles, which require a major modification of the particle content, the sterile neutrino does not entail any additional counterparts because it is gauge singlet. Sterile neutrinos can be produced from neutrino oscillations in the early universe in just the right amount to be the dark matter (Dodelson & Widrow 1994; Abazajian et al. 2001a, 2001b; Dolgov & Hansen 2002; Mapelli & Ferrara 2005; Abazajian 2005). If their mass exceeds 2 keV, they are sufficiently cold to explain the large-scale structure.

The discovery of neutrino oscillations points to the existence of some gauge singlets, at least those that make the right-handed counterparts of the active (left-handed) neutrinos. However, the number of *sterile* neutrinos is still unknown. Unless some neutrino experiments are wrong, the present data on neutrino oscillations cannot be explained without sterile neutrinos. Neutrino oscillations experiments measure the differences between the squares of neutrino masses, and the results are as follows: one mass squared difference is of the order of 10^{-5} (eV²), the other one is 10^{-3} (eV²), and the third is about 1 (eV²). Obviously, one needs more than three masses to get the three different mass splittings, which do not add up to zero. Since we know that there are only three active neutrinos, the fourth neutrino must be sterile. However, if the light sterile neutrinos exist, there is no compelling reason why their number should be limited to one. Some theoretical arguments favor at least three sterile neutrinos (Asaka et al. 2005). If there are three sterile neutrinos, they can help explain the matter-antimatter asymmetry of the universe (Asaka & Shaposhnikov 2005).

Oscillations to sterile neutrinos add an intriguing additional consequence to the search for a neutron star kick mechanism; the opportunity to use supernovae as laboratories to study particle physics. Other weakly interacting particles, for example, majorons, may cause the asymmetry as well (Farzan et al. 2005). Supernova asymmetries can be used to discover or constrain a class of weakly interacting particles with masses below 100 MeV. It is useful, therefore, to separate the details of a particular kick mechanism from its effects on the supernova and to perform a model-independent analysis of how the nonejecta kicks impact the rest of the supernova. This is the main goal of the present paper.

The neutrino-driven explosion mechanism has evolved considerably since its introduction by Colgate & White (1966). Although it is becoming increasingly accepted that convection above (and possibly within) the proto-neutron star can help make neutrino heating efficient enough to drive an explosion, the current state-of-the-art produces a range of results (Burrows

et al. 1995; Janka & Müller 1996; Mezzacappa et al. 1998; Fryer 1999; Fryer & Heger 2000; Fryer & Warren 2002, 2004; Buras et al. 2003; Walder et al. 2005). Over the past few years, a number of papers have studied ways to make the convection more vigorous, from asymmetries in the collapse (Burrows & Hayes 1996; Fryer 2004) to instabilities in the accretion shock and a possible vortical-acoustic instability (Blondin et al. 2003; Scheck et al. 2004). The neutrino-driven kicks have the effect of breaking the spherical symmetry of the overall explosion, which may help stir the material and strengthen the convection.

In this paper, we study the effects of the neutrino-oscillation kick mechanism on the core-collapse engine. We test its ability to help drive an explosion and study the observational implications of an explosion driven by the asymmetric emission from neutrinos. Section 2 describes our computational setup and the results of the simulations. We find that, under some conditions, neutrino-driven kicks can affect the explosion. In § 3, we study this effect and how it aids the explosion mechanism. We conclude with a discussion of the observational implications from these effects and how these observations constrain what we know about neutrino oscillations.

2. SIMULATIONS

All our simulations begin with the standard $15 M_{\odot}$ progenitor “s15s7b2” produced by Woosley & Weaver (1995). This progenitor is then mapped into three dimensions using a series of spherical shells. The entire evolution from collapse to explosion (if an explosion occurs) is modeled using SNSPH (Fryer et al. 2006). High-resolution simulations using this code develop convection almost immediately after bounce and produce delayed neutrino explosions 150 ms later. The effect of kicks driven by neutrino oscillations is small for these quick explosions.

For this paper, we focus on the effect these kicks can have on a marginal explosion. Although our simulations are meant to model generically how movement of the neutron star can affect the supernova explosion, we focus on a kick engine driven by sterile neutrinos. Sterile neutrinos are emitted with some anisotropy along the direction of the dipole magnetic field. If the neutron star period of rotation is low, this direction is almost constant on the timescales relevant for the shock formation. In a more realistic case of a rapid rotation about some other axis that is, generally, unrelated to the direction of the magnetic field, the thrust along the axis of rotation is nearly constant, while the orthogonal components average to zero. In either case, the recoil forces are applied to the nuclear matter well below the neutrinosphere. These forces make the matter above certain density move as a whole. For the purposes of our simulations we assume that the central region moves with a constant acceleration.

For the two variants of the pulsar kicks due to a sterile neutrino emission, it was shown by Kusenko & Segré (1997) and by Fuller et al. (2003), respectively, that the neutron star can acquire a speed of the order of 1000 km s^{-1} from the neutrino emission that lasts about 10 s. The average acceleration is, therefore, $a_{\text{Kick}} \sim 100 \text{ km s}^{-2}$. Although the onset of the kick may be delayed by the time evolution of the neutrino matter potential (Fuller et al. 2003), for a range of the neutrino masses and mixing angles this delay is less than 10 ms. The subsequent emission of sterile neutrinos is nearly constant over several seconds. It is appropriate, therefore, to model the kick by assuming that the core or the neutron star has a constant acceleration $a_{\text{Kick}} \sim 100 \text{ km s}^{-2}$.

The basic picture behind the convectively driven explosions can be described with a pressure-cooker analogy (Herant et al. 1994; Fryer 1999). Neutrinos from the proto-neutron star (heat

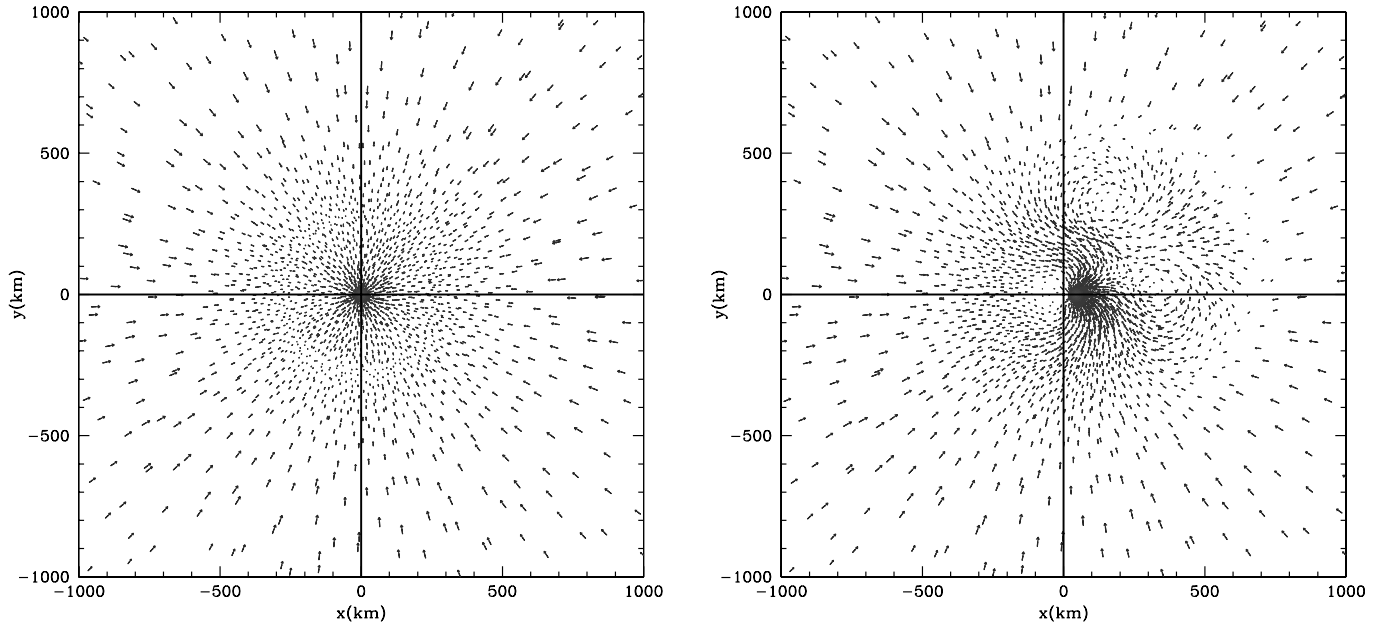


FIG. 1.—Comparison of the symmetric “HVisc0” (left) and kick “HVisc100” (right) models 90 ms after bounce. These plots show a slice of data centered on the $z = 0$ plane with the kick in the positive x -direction. Shading denotes entropy (dark is low, light is high) and the direction and length of arrows denote the direction and magnitude of the velocity. Note that the kicked model has developed some strong convection, which is pushing out the accretion shock. It ultimately develops into a strong explosion (Fig. 3). Primarily because of the low resolution, convection does not develop in the symmetric model and this model does not explode. [See the electronic edition of the Supplement for a color version of this figure.]

source) drive convection that pushes against the ram-pressure force of the infalling star (lid of the pressure cooker). Where the infalling material hits the upward flows of the convective region, an accretion shock forms. If the convection can drive this accretion shock outward, an explosion occurs (Fryer 1999). Hence, if we delay or damp out the convection, the star is less likely to explode and we can turn an explosion into a fizzle. We believe the differences in the convective modeling explain many of the differences between the simulations over the past decade.

We have made a series of modifications to delay convection, ultimately causing our zero-kick models to fail to produce supernova explosions. These modifications include switching the equation of state to reduce the initial postbounce entropy gradient to reducing the simulation resolution and increasing the artificial viscosity to damp out the initial perturbations. With these modifications, our spherically symmetric model does not produce an explosion, and at the end of the simulation, the shock radius has already begun to move inward (Fig. 1). Although this simulation does not explode, it straddles the explosion/fizzle boundary. Our models including strong neutrino-driven kicks develop much more convection (Fig. 1) and, as we shall see later in this section, ultimately produce asymmetric explosions. Before we discuss these results, let us review the modifications to the code that delayed the convection.

First, we effectively remove the coupled equation of state developed in Herant et al. (1994) by lowering the critical density for the Lattimer-Swesty (LS) equation of state (Lattimer & Swesty 1991) to 10^9 g cm^{-3} (from $10^{11} \text{ g cm}^{-3}$). A now-accepted error in the energy levels of the Lattimer-Swesty network leads to a slightly different density/temperature boundaries for abundance states (e.g., the α -particle peak; see F. X. Timmes et al. 2006, in preparation, for details). This can lead to very different entropy profiles after bounce. Figure 2 shows the entropy profile with the lowered critical density (dark dots) versus the coupled network (light dots) 40 ms after bounce (models Stan0 and HVisc0 from Table 1). The vertical lines correspond to the shock positions

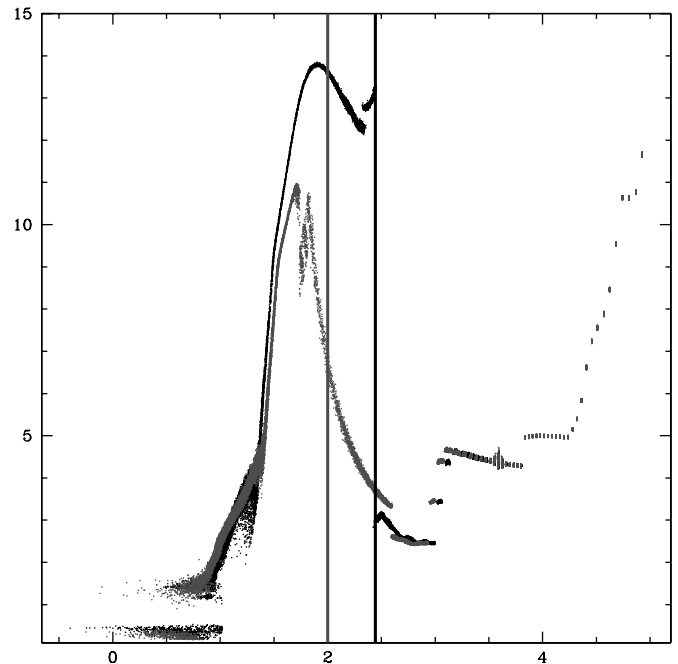


FIG. 2.—Entropy vs. radius 40 ms after bounce for models using the coupled equation of state from Herant et al. (1994) (light particles) compared with those using the Lattimer & Swesty (1991) equation of state down to low densities (dark particles). The vertical lines correspond to the positions of the accretion shock for these two models. Note that although the entropy from the coupled equation of state is lower than that using Lattimer-Swesty down to low densities, the entropy gradient out to the shock is much higher. This is more conducive to convection. The entropy gradient across the shock is also much more gradual in the case of the coupled equation of state. This is because nuclear dissociation and burning is playing a strong role in determining the entropy. [See the electronic edition of the Supplement for a color version of this figure.]

TABLE 1
SIMULATION PARAMETERS

Model	Particle Number	EOS ^a	α, β^b	$a_{\text{Kick}} (10^7 \text{ cm s}^{-2})$
StanHR0.....	399150	Her	1.5, 3.0	0
StanHR100.....	399150	Her	1.5, 3.0	100
Stan0.....	101685	Her	1.5, 3.0	0
MVisc10.....	101685	LS	2.0, 4.0	10
HVisc0.....	101685	LS	3.0, 6.0	0
HVisc100.....	101685	LS	3.0, 6.0	100

^a Her: The coupled equation of state described in Herant et al. (1994). LS: The equation of state using the Lattimer & Swesty (1991) equation of state down to densities of 10^9 g cm^{-3} .

^b The symbols α and β correspond to the standard SPH representation of the bulk and von Neuman–Richtmyer viscosities, respectively (Fryer et al. 2006).

for the coupled network (*light*) and lowered density model (*dark*). In the past, this difference in entropy profile has been attributed to either the simplified neutrino transport scheme of SNSPH or the inability of SNSPH to model shocks. We now believe that these differences are caused by equation-of-state differences. The smooth features of the entropy across the coupled equation of state shock occurs because nuclear burning is altering the entropy evolution. Although the entropy profile using the lowered critical density for the LS equation of state is less prone to convection, this alone is not enough to significantly alter the explosion.

Probably the most important modification was our use of low-resolution calculations (100,000–150,000 particles). Convective modes roughly below the smoothing-length size scale will not grow (A. Friedland et al. 2006, in preparation). By coarsening our resolution, many of the initial convective seeds do not grow and the convection is significantly delayed (Fig. 1). We have additionally increased the artificial viscosity of SPH while reducing the viscous heating to minimize overheating. The importance of these two changes can be seen in Table 2. The ultimate result of all these changes is that, for our symmetric runs, no explosion occurs. To drive an explosion, we must find a way to enhance the convection.

One way to enhance the convection is to drive larger scale convective modes either by producing more global asymmetries in the density or temperature or by weakening the ram pressure preventing the explosion. In the next section, we will review the role that neutrino-driven kicks can play in modifying the above list. Conservation of momentum requires that the proto–neutron star react to the asymmetric emission of sterile neutrinos, giving

the neutron star a kick. To mimic the effect of neutrino oscillations, we have modified the SNSPH code to include an artificial acceleration term to material that rises above a critical density. For our simulations, we used a critical density set to $10^{11} \text{ g cm}^{-3}$. The results do not change noticeably for critical densities lying between 10^{10} and $10^{14} \text{ g cm}^{-3}$ as this material is all ultimately part of the proto–neutron star and most of the proto–neutron star’s mass is at densities above $10^{14} \text{ g cm}^{-3}$. The velocities of the proto–neutron star using the entire range of critical densities lie within 10% of each other.

The two plots of the x - y plane comparing our “kicked” and symmetric models shows the difference in the shocks and the structure of the convection 92 ms after bounce. Figure 3 highlights the magnitude of this difference by plotting radial velocity versus radius for these two models at this same time. Figure 4 shows the high-viscosity kicked model (HVisc100) at the end of the simulation. The neutrino-driven kick led to an explosion with strong asymmetries in the direction of the kick. In the next section, we review the cause of this explosion revival and its accompanying asymmetry.

3. UNDERSTANDING THE ASYMMETRY

The explosion asymmetry in Figure 4 has a number of implications for observations of this neutrino-induced kick mechanism. Before we discuss these implications, we must first understand the cause of the asymmetry. A number of effects could lead to the asymmetry we observe: (i) material ahead of the moving neutron star is heated more efficiently by neutrinos diffusing out of the neutron star (or this material is heated by the moving neutron star); (ii) the ram pressure of the accretion shock is weakened ahead of the neutron star; or (iii) convection is driven by the motion of the neutron star (growing stronger ahead of the neutron star’s motion). These different options are summarized in Figure 5.

One can imagine two ways in which the material ahead of the moving neutron star could possibly be heated more effectively than the material in its wake: neutrino deposition or shocks from the moving neutron star. To test the neutrino deposition, Figure 6 shows the energy deposited by neutrinos above an assumed spherical gain region (Fryer 2004 found that the gain radius is actually larger in the direction of the proto–neutron star’s motion). It appears that there is more energy deposition for the moving neutron star. Indeed, the energy deposition for particles with $x > 0$ is $5.1 \times 10^{51} \text{ ergs s}^{-1}$ compared to $1.8 \times 10^{51} \text{ ergs s}^{-1}$ for particles with $x < 0$. For the symmetric simulation, the energies for particles with $x < 0$ and $x > 0$ are equal: $3.5 \times 10^{51} \text{ ergs s}^{-1}$. But this estimate is misleading. If we center the simulation about

TABLE 2
SIMULATIONS

Model	t_{Bounce}^a (ms)	ρ_{Bounce}^b ($10^{14} \text{ g cm}^{-3}$)	t_{exp}^c (ms)	$E_{\text{exp}, x>0}/E_{\text{exp}, x<0}^d$	P_x, P_y, P_z^e ($10^{40} \text{ g cm s}^{-1}$)
StanHR0.....	181	3.56	40	1.02	−0.04, −0.09, −0.36
StanHR100.....	178	3.42	40	1.00	0.08, 0.12, 0.36
Stan0.....	248	3.87	N/A	N/A	N/A
MVisc10.....	298	4.04	>300	N/A	N/A
HVisc0.....	208	3.66	N/A	N/A	N/A
HVisc100.....	208	3.86	90	6.54	5.4, 0.96, 0.11

^a Time between the onset of collapse of the S157B2 progenitor to bounce.

^b Core density at bounce.

^c Time after bounce when the explosion shock has reached 500 km. “N/A” refers to models that do not explode.

^d Ratio of explosion energies for all particles with $x > 0$ divided by those particles with $x < 0$. The explosion energy is defined as the kinetic energy of those particles with radial velocities greater than 0.

^e Total momentum of the particles with density less than $10^{12} \text{ g cm}^{-3}$.

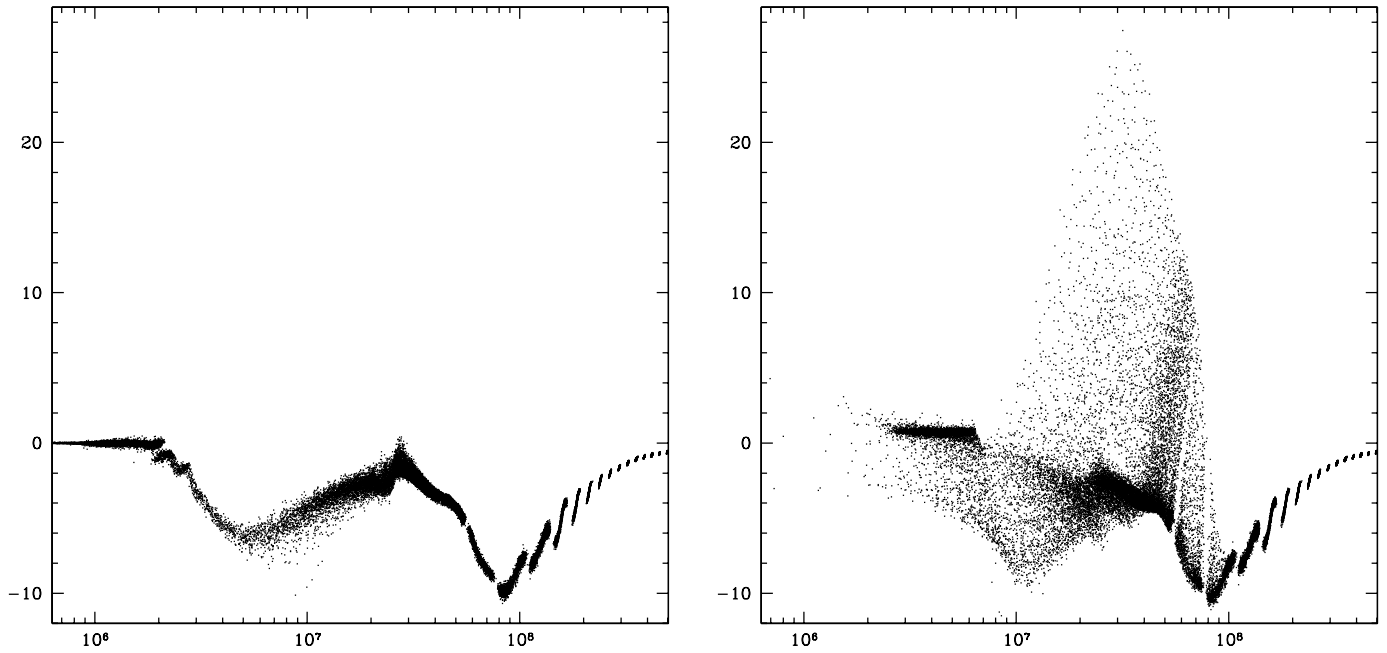


FIG. 3.—Radial velocity vs. radius for our symmetric (HVisc0) and kicked (HVisc100) models, showing clearly the lack of convection in the symmetric simulation in stark contrast to the convection that has developed in the kicked model. For all practical purposes, the symmetric model is behaving as one might expect in a one-dimensional simulation.

the center of the neutron star, the energy deposition for particles $x - x_{\text{NS}} > 0$ is within 1% of the deposition for particles with $x - x_{\text{NS}} < 0$. It is unlikely that asymmetric heating is causing the explosion asymmetry. The kinetic energy of the neutron star on the matter also is a minor effect; the total energy deposited by

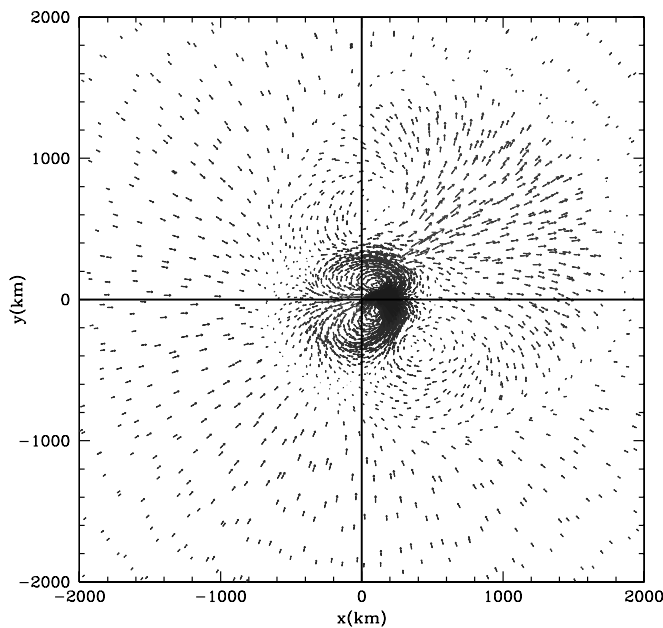


FIG. 4.—Slice of the kicked simulation “HVisc100” 160 ms after bounce. An explosion has been launched and, where it is strongest, has now nearly reached 2000 km. The explosion ejecta is strongest in roughly the *same* direction as the neutron star. Because the explosion ejecta is driven by convection, and the seeds for this convection are building on small asymmetries in the collapsing core, the fastest moving ejecta is not exactly aligned with the motion of the kick. Ejecta-driven kicks predict the exact opposite—the ejecta moves in the opposite direction to the neutron star. [See the electronic edition of the Supplement for a color version of this figure.]

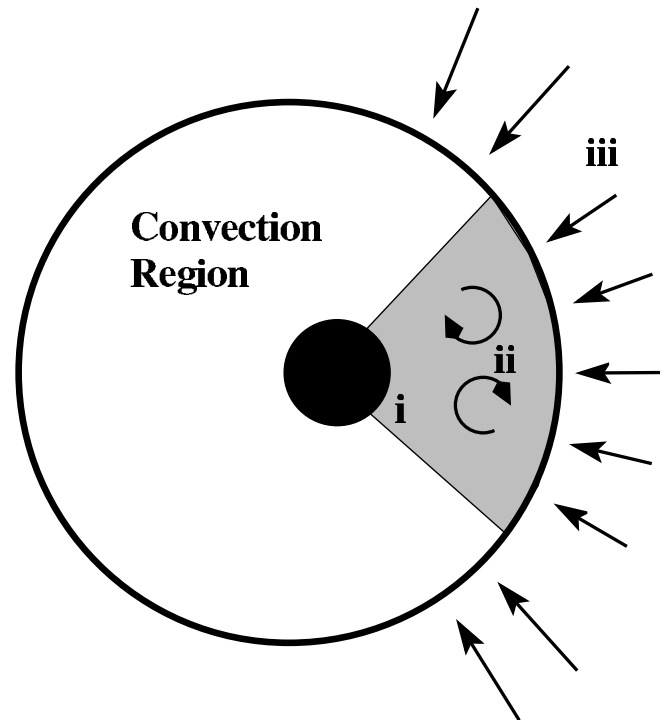


FIG. 5.—Possible causes for the ejecta asymmetry: (i) asymmetric neutrino heating or ram-heating caused by the motion of the proto-neutron star; (ii) weakened pressure at the accretion shock; or (iii) convection seeded by the motion of the proto-neutron star (possibly caused by minor effects of the previous two effects). Our analysis suggests that this latter cause is indeed the cause of the ejecta asymmetry in our exploding models. [See the electronic edition of the Supplement for a color version of this figure.]

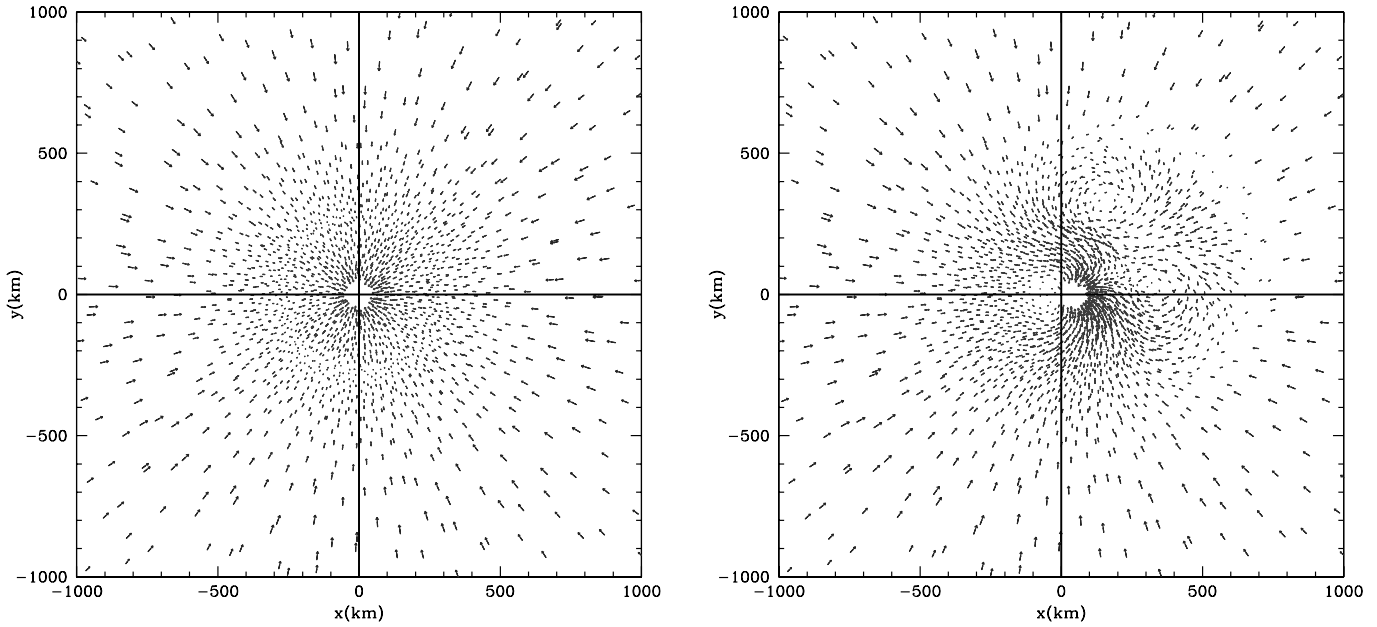


FIG. 6.—Slices of our symmetric (HVisc0) and kicked (HVisc100) models colored by the heating from neutrinos. The symmetric model exhibits no asymmetry in its net heating. Although there is more heating in the positive x -direction for the asymmetric model, if we use the center of our neutron star as the zero point, the neutrino heating for particles with $x - x_{\text{NS}} > 0$ equals that of the particles with $x - x_{\text{NS}} < 0$. [See the electronic edition of the Supplement for a color version of this figure.]

motion of the neutron star is less than 0.01% of the total matter energy.

Alternatively, the ram pressure of the infalling shock could be diminished on the edge leading the neutron star motion. But a study of our shocks shows that the pressure of the accretion shock on the leading and trailing edges do not differ by more

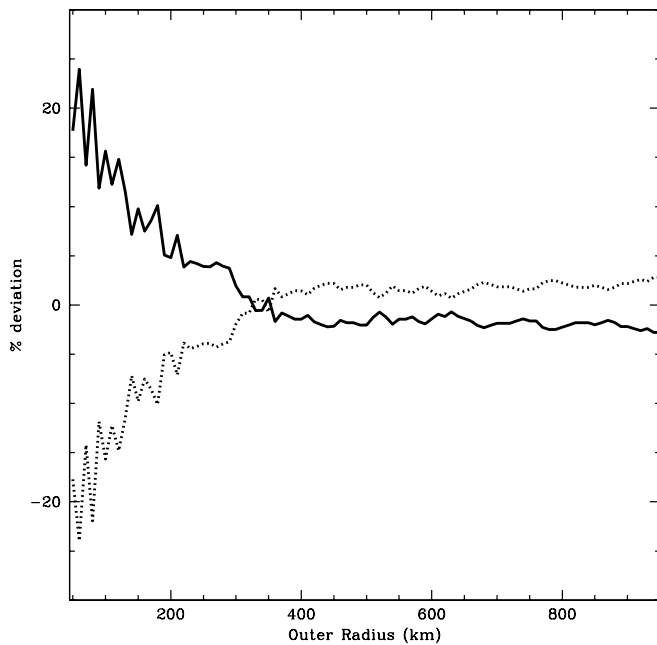


FIG. 7.—Percentage deviation from the mean of the mass as a function of radial bins (where the zero point in the radius is determined by the center of the neutron star) 75 ms after bounce. The solid line denotes the mass in a 15° cone leading the neutron star, the dotted line denotes the mass of a similar cone trailing the neutron star. Out to roughly 300 km, there is more mass ahead of the neutron star than the mean as it piles up against the neutron star. In the wake, the mass is below the mean. This mass increase is nearly 20% near the neutron star's surface. Beyond 300 km, the fact that the center of the neutron star is off of the center of the collapsing star means that the density ahead of the neutron star is lower, and the total mass is lower.

than a few percent. What is different is that the mass in the region between the accretion shock and the proto-neutron star is higher in front of the shock than behind; the effect of the neutron star's bow shock and wake as it moves through the collapsing star. Figure 7 shows the relative mass in a 15° cone leading the neutron star and trailing the neutron star as a function of radial bins out from the neutron star. Below 300 km, the mass is enhanced in front of the neutron star. If the neutron star

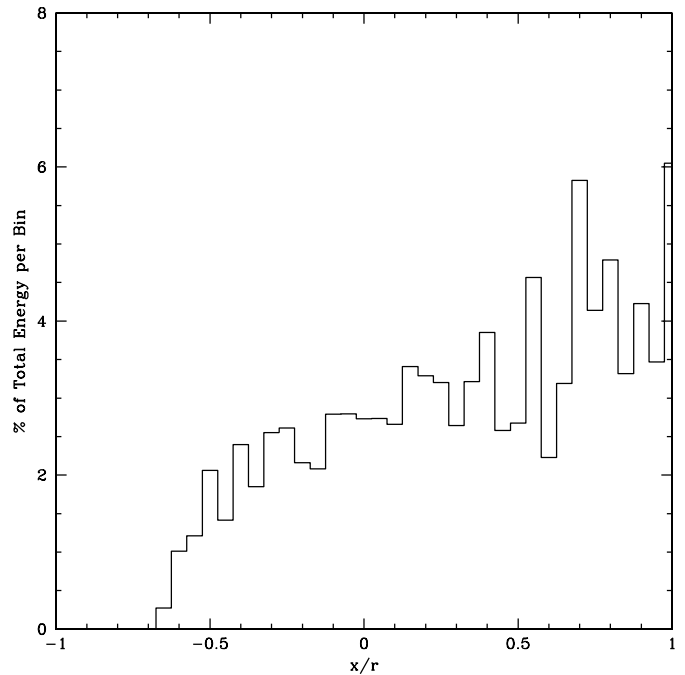


FIG. 8.—Percent of total energy per angular bin as a function of angle (x position over radius) for mass 70–110 km from the center of the proto-neutron star 75 ms after bounce. In this plot we see just how important the mass pile-up shown in Figure 7 is for the energy in this region. 70% of the total energy is ahead of the moving neutron star (the neutron star is moving in the positive x -direction), peaking directly ahead of the neutron star's motion.

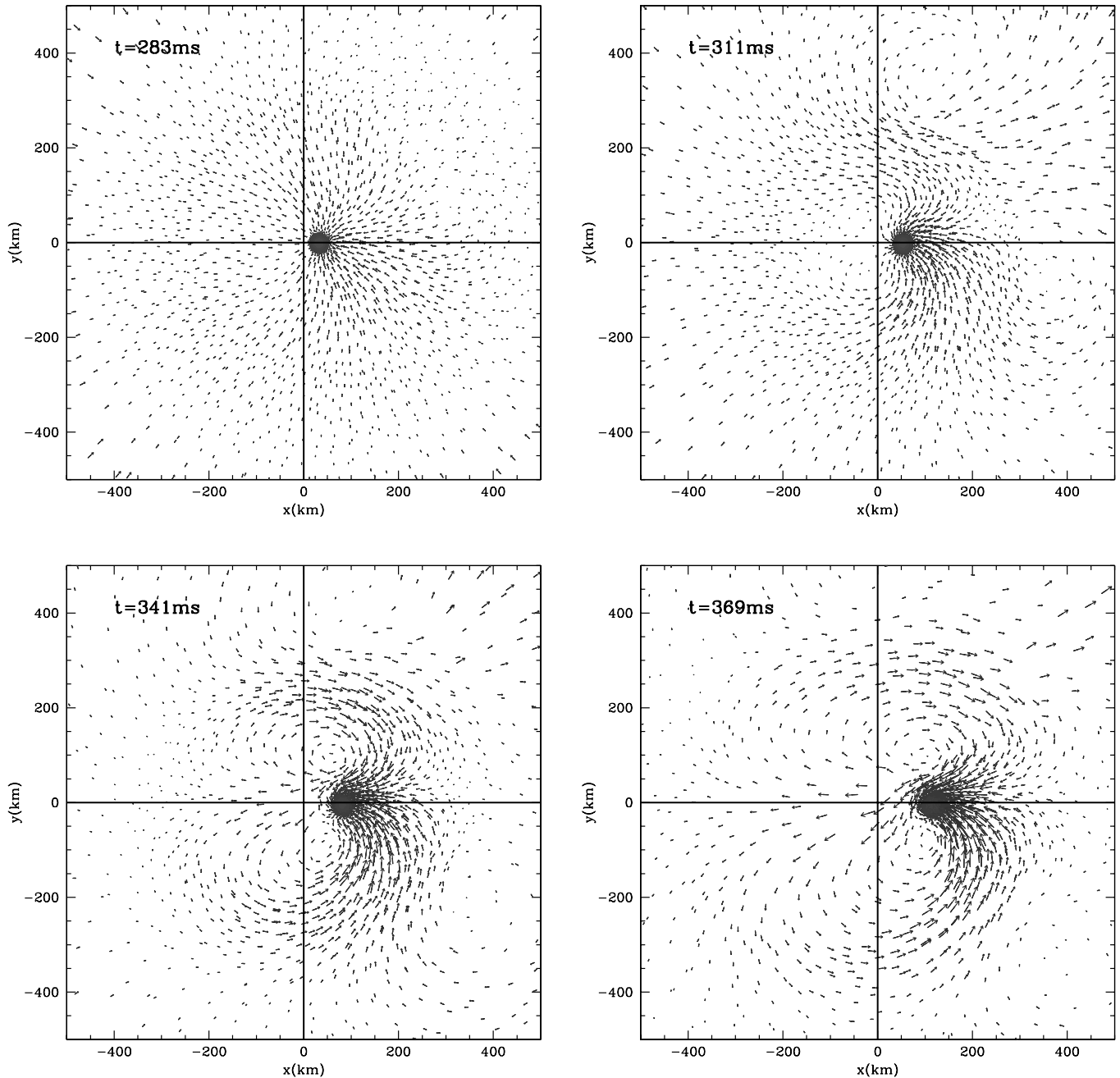


FIG. 9.—Four snapshots showing slices of the x - y plane of the HVISC100 simulation. These plots show a slice of data centered on the $z = 0$ plane with the kick in the positive x -direction. Shading denotes density (*dark is low, light is high*) and the direction and length of arrows denote the direction and magnitude of the velocity. These plots show the development of the instability seeded by the motion of the neutron star. [See the electronic edition of the Supplement for a color version of this figure.]

were moving supersonically, this would be the bow shock. Behind the neutron star, in its wake, the density is lowered. Beyond 300 km, the density is lower ahead of the neutron star. This occurs because the neutron star is moving through the collapsing star and is hitting the lower density layers of the star in front of it.

This effect helps build an explosion (and an explosion asymmetry) in two ways. First, the total energy in the budding convective region (the region between the proto-neutron star and the infalling shock) is much larger ahead of the proto-neutron star than behind. This is simply a restatement of the fact that the mass is piling up in front of the proto-neutron star. Figure 8 shows the energy distribution of matter in a shell 70–110 km away from the proto-neutron star as a function of angle. From Figure 8 we

clearly see the effect of this mass pile-up. Over 70% of the energy is in the forward direction, ahead of the proto-neutron star, and it is peaked directly in front of the neutron star's motion. The region above the neutron star already has a negative entropy gradient and, hence, is subject to Rayleigh-Taylor instabilities. For our model, these instabilities grow to slowly to produce an explosion. The increased energy in the forward direction helps seed and grow these instabilities, producing the strong convection we see in the simulations. Figure 9 shows the growth of this instability over four snapshots in time.

Second, because the density of the infalling material is lower ahead of the neutron star, the shock will experience a lower pressure when it reaches this point, making it easier to push the shock forward and drive an explosion. We believe these effects,

the stimulation of convection, turns the “fizzle” into an explosion. However, if the neutron star kick is not strong enough (as was the case with our lowered acceleration—MVisc10), the pile-up is insubstantial, and the kick does not produce an explosion. In a more borderline case, or if we follow the collapse further, this slower acceleration may well drive an explosion.

4. IMPLICATIONS

We have presented the results of six core-collapse supernova calculations (a total of 250,000 processor hours) studying the effects of asymmetric neutrino emission. If convection occurs without delay and the explosions are quick, neutrino-driven kicks do not significantly alter the supernova explosion. By lowering our resolution and damping out convection, we are able to produce “fizzles” (nonexploding stellar collapse models). In this scenario, neutrino-driven kicks are able to seed and drive convection, ultimately producing an explosion. The resultant explosions are asymmetric (Fig. 4). In the case of our HVisc100 model, the explosion is more than 6 times more energetic in the direction of the neutron star’s motion. Note, however, that we only found explosions for very fast accelerations. Our lowered acceleration (MVisc10) did not produce an explosion in the 300 ms after bounce. Even so, we believe a low-acceleration version of this neutrino-driven mechanism will drive an asymmetry for extremely delayed supernova mechanisms, e.g., Burrows et al. (2005). But remember that neutrino-driven kicks can exist without any outward effect on the supernova explosion if the explosion occurs early.

Neutrino-driven kick mechanisms have several distinguishing features that allow us to differentiate them from ejecta-driven kick mechanisms. First, the neutrino-driven kicks must occur during the time of the neutrino emission, that is during the first 10 s after the supernova. As was emphasized by Spruit & Phinney (1998), a kick mechanism of this sort should produce an alignment of the pulsar velocity with the axis of rotation. This is because the components of the kick orthogonal to the axis of rotation average to nearly zero after many rotations the pulsar makes in the first 10 s. Johnston et al. (2005) have presented strong observational evidence for such an alignment, which appears to lend further support to the neutrino-driven kick mechanisms.⁴ Spruit & Phinney (1998) have also pointed out that a kick mechanism of this kind can explain both the proper motions and the rapid rotations of pulsars.

⁴ We note in passing that no correlation between the magnitude of the velocity and the strength of the surface magnetic field is expected from this mechanism (Kusenko 2004). The B - v correlation is not expected because the surface magnetic field of a million year old pulsar is not a good representative of the interior magnetic field during the first 10 s (Duncan & Thompson 1992; Thompson & Duncan 1993).

It is conceivable, although by no means automatic, that some ejecta-driven mechanisms could also produce an alignment of the kick with the pulsar’s axis of rotation. However, by the momentum conservation, the ejecta should recoil in the direction opposite of the pulsar motion. If neutrino-driven kicks help drive the supernova explosion, the explosion ejecta is strongest in the same direction of the motion of the neutron star. This means that there should be more mixing in the direction of the neutron star’s motion for these neutrino-driven kicks, and elements like nickel will mix further out in this direction (Hungerford et al. 2005). If one believes the compact object identification of Sgr A East (Park et al. 2005), this extended mixing in the direction of the neutron star kick has already been observed. This observation is circumstantial, but it does show the possibility of distinguishing between these two kick mechanisms. We stress that this is only valid if the neutrino-driven mechanism is responsible for the supernova explosion (it is not valid if the explosion is quick).

An additional independent confirmation of the neutrino-driven kicks can come from observations of the gravity waves. It is well-known that a departure from spherical symmetry is necessary for generating gravitational waves. A neutron star emitting neutrinos anisotropically, while rotating around some axis that is not aligned with the direction of the anisotropy, creates a source of gravity waves observable by Advanced LIGO and *LISA* in the event of a nearby supernova (Loveridge 2004). The signal discussed by Loveridge (2004) is caused by the rotating ray of overdensity in the neutrino distribution. Gravity waves may also be sourced by anisotropic distribution of oscillating neutrinos deep inside the neutron star (Cuesta 2002).

5. CONCLUSIONS

To summarize, we have shown that pulsar kick mechanisms based on anisotropic emission of neutrinos or other weakly interacting particles from the cooling neutron star can increase the energy gained by the shock, hence improving the prospects for a successful explosion. A distinguishing feature of this class of mechanisms is asymmetric explosion enhanced in the direction of the motion of the neutron star.

The work of C. L. F. was funded in part under the auspices of the US Department of Energy, and supported by its contract W-7405-ENG-36 to Los Alamos National Laboratory, and by a DOE SciDAC grant DE-FC02-01ER41176. The work of A. K. was supported in part by the US Department of Energy grant DE-FG03-91ER40662 and by NASA grants ATP02-0000-0151 and ATP03-0000-0057.

REFERENCES

- Abazajian, K. 2005, preprint (astro-ph/0511630)
 Abazajian, K., Fuller, G. M., & Patel, M. 2001a, *Phys. Rev. D*, 64, 023501
 Abazajian, K., Fuller, G. M., & Tucker, W. H. 2001b, *ApJ*, 562, 593
 Arras, P., & Lai, D. 1999, *Phys. Rev. D*, 60, 3001
 Arzoumanian, Z., Chernoff, D. F., & Cordes, J. M. 2002, *ApJ*, 568, 289
 Asaka, T., Blanchet, S., & Shaposhnikov, M. 2005, preprint (hep-ph/0503065)
 Asaka, T., & Shaposhnikov, M. 2005, *Phys. Lett. B*, 620, 17
 Barkovich, M., D’Olivo, J.-C., Montemayor, R., & Zanella, J. F. 2002, *Phys. Rev. D*, 66, 123005
 Barkovich, M., D’Olivo, J.-C., & Montemayor, R. 2004, *Phys. Rev. D* 70, 043005
 Blandford, R. D., Applegate, J. H., & Hernquist, L. 1983, *MNRAS*, 204, 1025
 Blondin, J. M., Mezzacappa, A., & DeMarino, C. 2003, *ApJ*, 584, 971
 Buras, R., Rampf, M., Janka, H.-T., & Kifonidis, K. 2003, *Phys. Rev. Lett.*, 90, 1101
 Burrows, A., & Hayes, J. 1996, *Phys. Rev. Lett.*, 76, 352
 Burrows, A., Hayes, J., & Fryxell, B. A. 1995, *ApJ*, 450, 830
 Burrows, A., Livne, E., Dessart, L., Ott, C., & Murphy, J. 2005, *ApJ*, submitted (astro-ph/0510687)
 Chugai, N. N. 1984, *Pis’m’a Astron. Zh.* 10, 210 (English trans. in *Soviet Astron. Lett.* 10, 87)
 Colgate, S. A., & White, R. H. 1966, *ApJ*, 143, 626
 Cordes, J. M., & Chernoff, D. F. 1998, *ApJ*, 505, 315
 Cuesta, H. J. 2002, *Phys. Rev. D*, 65, 061503
 Dodelson, S., Widrow, L. M. 1994, *Phys. Rev. Lett.*, 72, 17
 Dolgov, A. D., & Hansen, S. H. 2002, *Astropart. Phys.*, 16, 339
 Dorofeev, O. F., Rodionov, V. N., & Ternov, I. M. 1985, *Soviet Astron. Lett.*, 11, 123
 Duncan, R. C., & Thompson, C. 1992, *ApJ*, 392, L9
 Farzan, Y., Gelmini, G., & Kusenko, A. 2005, *Phys. Lett. B*, 621, 22

- Fryer, C. L. 1999, *ApJ*, 522, 413
———. 2004, *ApJ*, 601, L175
Fryer, C. L., Burrows, A., & Benz, W. 1998, *ApJ*, 496, 333
Fryer, C. L., & Heger, A. 2000, *ApJ*, 541, 1033
Fryer, C. L., Rockefeller, G., & Warren, M. S. 2006, *ApJ*, in press (astro-ph/0512532)
Fryer, C. L., & Warren, M. S. 2002, *ApJ*, 574, L65
———. 2004, *ApJ*, 601, 391
Fuller, G. M., Kusenko, A., Mocioiu, I., & Pascoli, S. 2003, *Phys. Rev. D*, 68, 103002
Gott, J. R. I., Gunn, J. E., & Ostriker, J. P. 1970, *ApJ*, 160, L91
Harrison, E. R., & Tademaru, E. 1975, *ApJ*, 201, 447
Herant, M., Benz, W., & Colgate, S. A. 1992, *ApJ*, 395, 642
Herant, M., Benz, W., Hix, W. R., Fryer, C. L., & Colgate, S. A. 1994, *ApJ*, 435, 339
Hungerford, A., Fryer, C. L., & Rockefeller, G. 2005, *ApJ*, 635, 487
Janka, H.-T., & Müller, E. 1996, *A&A*, 306, 167
Kouveliotou, C. et al. 1999, *ApJ*, 510, L115
Kusenko, A. 2004, *Int. J. Mod. Phys. D*, 13, 2065
Kusenko, A., & Segrè, G. 1996, *Phys. Rev. Lett.*, 77, 4872
———. 1997, *Phys. Lett. B*, 396, 197
Kusenko, A., Segrè, G., & Vilenkin, A. 1998, *Phys. Lett. B*, 437, 359
Johnston, S., Hobbs, G., Vigeland, S., Kramer, M., Weisberg, J. M., & Lyne, A. G. 2005, *MNRAS*, 364, 1397
Lai, D., Chernoff, D. F., & Cordes, J. M. 2001, *ApJ*, 549, 1111
Lattimer, J. M., & Swesty, F. D. 1991, *Nucl. Phys. A*, 535, 331
Loveridge, L. C. 2004, *Phys. Rev. D*, 69, 024008
Mapelli, M., & Ferrara, A. 2005, *MNRAS*, 364, 2
Mezzacappa, A., Calder, A. C., Bruenn, S. W., Blondin, J. M., Guidry, M. W., Strayer, M. R., & Umar, A. S. 1998, *ApJ*, 495, 911
Park, S., et al. 2005, *ApJ*, 631, 964
Scheck, L., Plewa, T., Janka, H.-T., Kifonidis, K., & Müller, E. 2004, *Phys. Rev. Lett.*, 92, 1103
Socrates, A., Blaes, O., Hungerford, A., & Fryer, C. L. 2005, *ApJ*, 632, 531
Spruit, H. C., & Phinney, E. S. 1998, *Nature*, 393, 139
Thompson, C., & Duncan, R. C. 1993, *ApJ*, 408, 194
Trimble, V., & Rees, M. J. 1971, *ApJ*, 166, L85
Vilenkin, A. 1995, *ApJ*, 451, 700
Walder, R., Burrows, A., Ott, C. D., Livne, E., Lichtenstadt, I., & Jarrah, M. 2005, *ApJ*, 626, 317
Woosley, S. E., & Weaver, T. A. 1995, *ApJS*, 101, 181